

POS0011

## The Strain Distribution on Femoral Bone Inserted Hip Prosthesis and Intramedullary Nail under Dynamic Loading Condition

Kittigorn Chalernphon<sup>1</sup>, Prompong Anuchitchanchai<sup>2</sup>, Kitti Aroonjarattham<sup>2</sup>, Chompunut Somtua<sup>1,3</sup> and Panya Aroonjarattham<sup>1,\*</sup>

<sup>1</sup> Department of Mechanical Engineering, Faculty of Engineering, Mahidol University, Nakornpathom, Thailand, 73170

<sup>2</sup> Department of Orthopaedics, Faculty of Medicine, Burapha University, Chonburi, Thailand, 20131

<sup>3</sup> Department of Mechanical Engineering, Faculty of Engineering, Bangkok Thonburi University, Bangkok, Thailand, 10170

\* Corresponding Author: panya.aro@mahidol.ac.th

### Abstract

The dynamic walking and stair-climbing condition act as the continuous load that similar to the daily activities. This study aims to evaluate the strain distribution on the femoral bone, femoral bone inserted hip prosthesis and femoral bone inserted intramedullary nail under dynamic loading condition and to compare the effect of dynamic loading to the bone-implant with static condition. The difference of the maximum equivalent of total strain between static and dynamic loading was 0% on femoral bone model, 0.02% on femoral bone inserted hip prosthesis and 9.52% on femoral bone inserted intramedullary nail. The maximum von Mises stress on hip prosthesis and intramedullary nail had difference 0% and 7.71% between static and dynamic condition respectively. The dynamic loading condition had effect to the femoral bone inserted intramedullary nail.

**Keywords:** Dynamic Loading, Femoral Bone, Hip Prosthesis and Intramedullary Nail.

### 1. Introduction

Finite element analysis was a popularly used to analyze the stress and strain distribution on the bone-implant [1-3]. Static condition was used the peak load from electromyography (EMG) data to analyze the model by finite element method [4, 5]. Therefore, this study aims to use the finite element method to analyze stress distribution on two basic devices as hip prosthesis and intramedullary nail to represent the load bearing and load sharing devices and strain distribution on the femoral bone under dynamic walking condition to compare with the result from static walking condition. Dynamic loading condition was continuous load that should be giving the result difference from static analysis. The result will use to evaluate the effect of dynamic loading to the bone-implant effect the size of implant.

### 2. Material and Methods

#### 2.1 Three-dimensional Model

##### 2.1.1 Femoral bone

Three-dimensional model of femur was scanned by the computed tomography (CT) scanner and was reconstructed by ITK-SNAP program. The model was divided into four main parts as proximal cortex, proximal cancellous, distal cortex and distal cancellous as shown in Fig. 1.

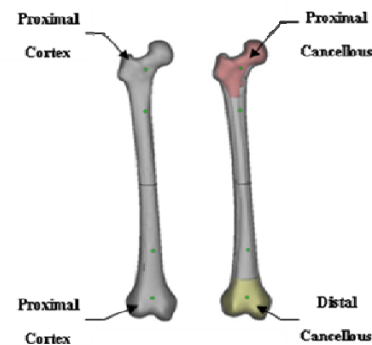


Fig. 1 Three-dimensional model of femoral bone

##### 2.1.2 Hip prosthesis

Hip prosthesis was divided in two main types as cemented and cementless model. The cementless hip prosthesis widely used in Thai patient, was used in this study. The three-dimensional model of hip prosthesis was created from SolidWorks software with actual dimension as shown in Fig. 2.



Fig. 2 Three-dimensional model of hip prosthesis.

##### 2.1.3 Intramedullary nail

Intramedullary nail (Universal femoral nail, Synthes) was created from SolidWorks software with actual dimension. The screw fixation was assumed as a cylindrical shape because the maximum von Mises stress had occurred on the nail and the core of screw

## POS0011

higher than on the thread. The three-dimensional model of intramedullary nail and four screws fixation were shown in Fig. 3.



Fig. 3 Three-dimensional model of intramedullary nail and four screws fixation.

### 2.2 Virtual Simulation

#### 2.2.1 Hip prosthesis

The hip stem was placed to the center of the medullary canal and fit with the hollow of the femur as shown in Fig. 4.

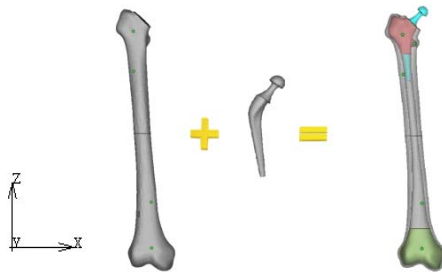


Fig. 4 Femur inserted hip prosthesis.

#### 2.2.2 Intramedullary nail

Intramedullary nail was inserted to the medullary canal to fix the fracture gap, was defined as initial connective tissue. The axis of intramedullary nail and medullary canal must be coincidence with the best fit position as shown in Fig. 5.

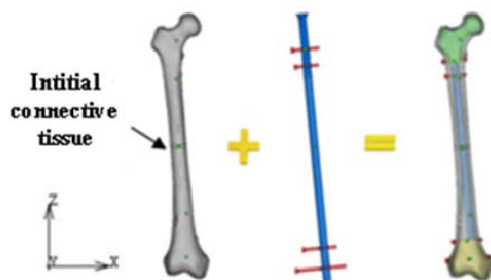


Fig. 5 Intramedullary nail was inserted in femoral bone.

### 2.3 Material Properties

All models were assumed homogeneous material, linear elastic and isotropic property [1-5]. Material properties of cortical bone, cancellous bone, titanium alloy, initial connective tissue and SS AISI 316 were shown in Table. 1.

Table. 1 Material properties of all models [6, 7].

Material	Young's modulus (MPa)	Poisson's ratio
Cortical bone	14,000	0.3
Cancellous bone	600	0.2
Intitial connective tissue	3	0.4
Titanium Aolly	110,000	0.3
SS AISI 316L	200,000	0.3

### 2.4 Boundary Condition

Walking condition consisted of 2 main loads as: body weight was act on the femoral head and muscular forces were act on the proximal part [8]. This study was evaluated under two conditions as static and dynamic loading condition by preparation as follows:

#### 2.4.1 Static Condition

The magnitude of muscular forces was shown in Table. 2.

Table. 2 Load profile under static walking condition (Body weight = 836N) [9]

Force	$F_x$	$F_y$	$F_z$
Hip contact	-54.0	-32.8	-229.2
Intersegmental resultant	-8.1	-12.8	-78.2
Abductor	58.0	4.3	86.5
Tensor fascis latae, proximal part	7.2	11.6	13.2
Tensor fascis latae, distal part	-0.5	-0.7	-19.0
Vastus lateralis	-0.9	18.5	-92.9

#### 2.4.2 Dynamic condition

The dynamic condition was analyzed the hip contact force and the muscular force varied with time during the entire load cycle. The dynamic walking was shown the hip contact force and the muscular force in Fig. 6 - 10.

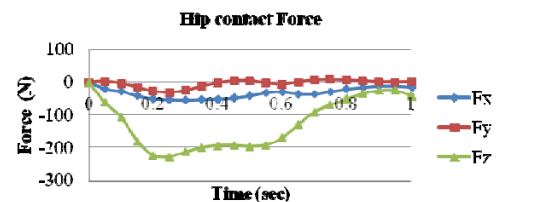


Fig. 6 The hip contact force under dynamic walking condition [9]

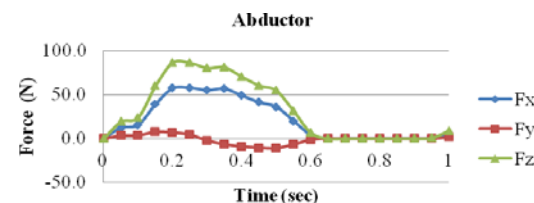


Fig. 7 The abductor force under dynamic walking condition [9]

## POS0011

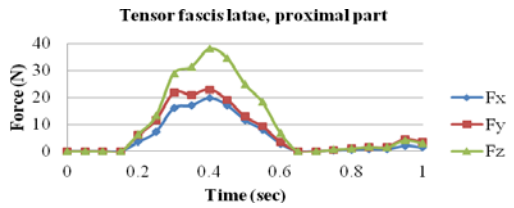


Fig. 8 The tensor fascis latae, proximal part force under dynamic walking condition [9]

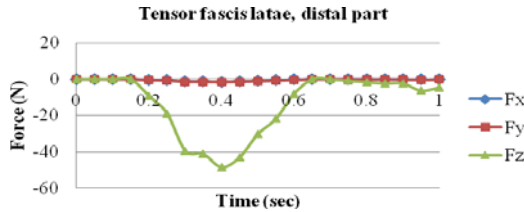


Fig. 9 The tensor fascis latae, distal part force under dynamic walking condition [9]

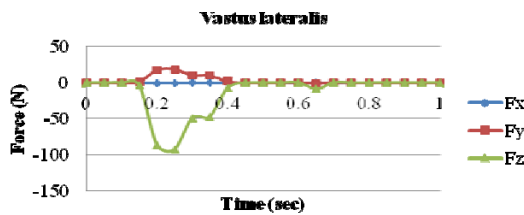


Fig. 10 The vastus lateralis force under dynamic walking condition [9]

The position of muscular force was determined from Heller M.O., *et al* [10]. Body weight was act at P0. The hip contact force and intersegmental resultant were act at P1. The abductor, tensor fascis latae proximal part and tensor fascis latae distal were act at P2. The vastus lateralis was act at P3. The position of P0, P1, P2 and P3 were shown in Fig. 11.

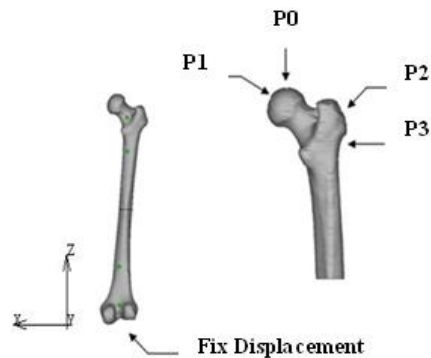


Fig. 11 The position of loading on the proximal femur.

### 3. Result

All models were evaluated by finite element method under static and dynamic walking condition to obtain the von Mises stress and the equivalent of total

strain distribution on the model. Femoral bone was analyzed the maximum equivalent of total strain and hip prosthesis and intramedullary nail were analyzed the maximum von Mises stress. The result was shown in each case respectively.

#### 3.1 The equivalent of total strain on femoral bone

Bone model was analyzed under static walking and dynamic walking condition. The equivalent of total strain distribution on the bone was shown in Fig. 12.

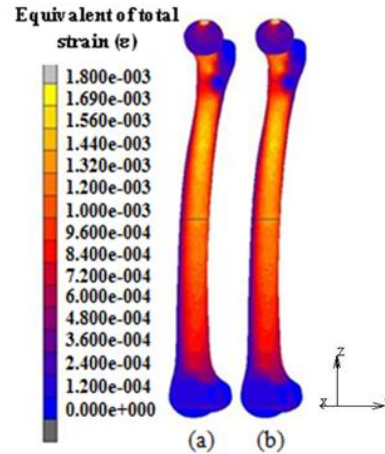


Fig. 12 The equivalent of total strain distribution on the medial side of femoral bone under: (a) Static walking and (b) Dynamic walking.

#### 3.2 The equivalent of total strain on femoral bone inserted hip prosthesis

Bone model was analyzed under static walking and dynamic walking condition. The equivalent of total strain distribution on the bone inserted hip prosthesis was shown in Fig. 13.

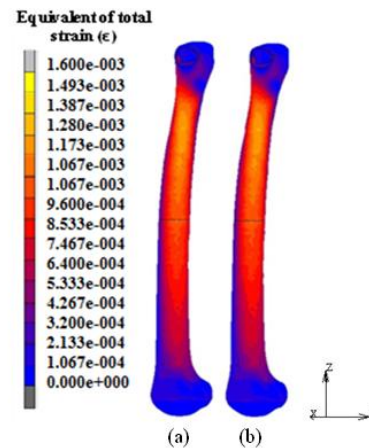


Fig. 13 The equivalent of total strain distribution on the medial side of femoral bone inserted hip prosthesis under: (a) Static walking and (b) Dynamic walking.

## POS0011

### 3.3 The equivalent of total strain on femoral bone inserted intramedullary nail

Bone model was analyzed under static walking and dynamic walking condition. The equivalent of total strain distribution on the bone inserted intramedullary nail was shown in Fig. 14-15 for proximal part and distal part respectively.

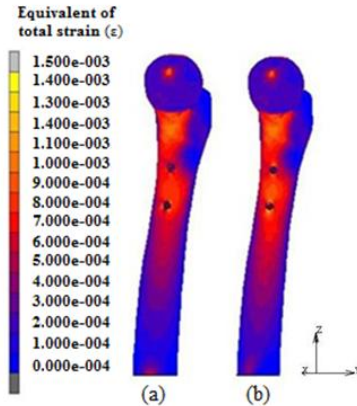


Fig. 14 The equivalent of total strain distribution on the medial side of proximal femur inserted intramedullary nail under: (a) Static walking and (b) Dynamic walking.

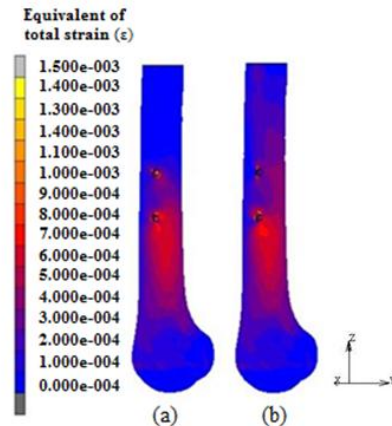


Fig. 15 The equivalent of total strain distribution on the medial side of distal femur inserted intramedullary nail under: (a) Static walking and (b) Dynamic walking.

### 3.4 The von Mises stress on hip prosthesis

Hip prosthesis was analyzed under static walking and dynamic walking condition. The stress distribution on hip prosthesis was shown in Fig. 16.

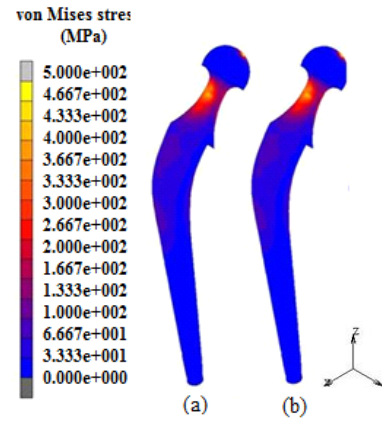


Fig. 16 The stress distribution on hip prosthesis under: (a) Static walking and (b) Dynamic walking.

### 3.5 The von Mises stress on intramedullary nail

Intramedullary nail was analyzed under static walking and dynamic walking condition. The stress distribution on hip prosthesis was shown in Fig. 17.

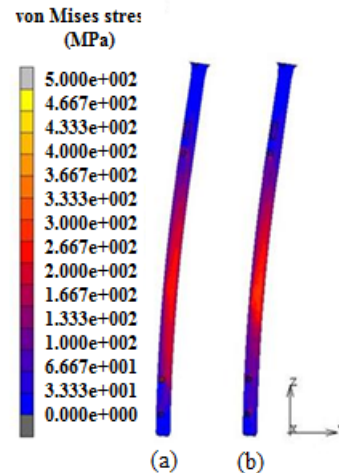


Fig. 17 The stress distribution on intramedullary nail under: (a) Static walking and (b) Dynamic walking.

## 4. Discussion

The strain distribution on femoral bone and the stress distribution on the implants were compared to evaluate the effect of dynamic loading. All models were discussed as follow:

### 4.1 Femoral bone

The femoral bone was broken when the strain distribution on the bone equal or higher than 25,000 microstrain ( $\mu\epsilon$ ) [11-13]. All models was evaluated the maximum equivalent of total strain on femoral bone at the medial side, which was received the compression load, to compare between static and dynamic condition as shown in Table. 3.



## POS0011

Table. 3 The maximum equivalent of total strain on femoral bone, femoral bone inserted hip prosthesis and femoral bone inserted intramedullary nail ( $\mu\epsilon$ ).

Bone	The maximum equivalent of total strain ( $\mu\epsilon$ )		Difference (%)
	Static Walking	Dynamic Walking	
Femoral bone	1,497.20	1,497.20	0%
Femoral bone inserted hip prosthesis	1,252.70	1,252.90	0.02%
Femoral bone inserted intramedullary nail	1,029.10	1,127.10	9.52%

Femoral bone inserted intramedullary nail had the difference of maximum equivalent of total strain between static and dynamic loading higher than the other model that shown the dynamic loading affect bone inserted load sharing device.

### 4.2 Hip prosthesis

All model of hip prosthesis had the maximum von Mises stress less than the yield strength of titanium alloy [14, 15]. The difference of maximum von Mises stress between static and dynamic condition was 0% that shown the dynamic loading did not effect to the load bearing device.

### 4.3 Intramedullary nail

Intramedullary nail was a surgical treatment of dia-metaphyseal fracture, which was placed within the medullary canal to stabilize the fracture fragment during the healing process. All cases had the maximum von Mises stress less than the yield strength of SS AISI 316L [16]. The difference of maximum von Mises stress between static and dynamic condition was 7.71% that shown the dynamic loading effect to the load sharing device.

## 5. Conclusion

Static loading can use to analyze the femoral bone and femoral bone inserted hip prosthesis because the difference of maximum equivalent of total strain was 0% when compare with dynamic loading. The maximum von Mises stress on the hip prosthesis had the same value under both condition but the bone inserted intramedullary nail should be analyzed under dynamic loading condition because this model had the fracture gap that made the bone unstable which affect the load varied with time.

## 6. Acknowledgement

The authors wish to thank the Faculty of Medicine, Burapha University and Biomechanics Analysis and Orthopedic Device Design Laboratory (B-AODD LAB), Department of Mechanical Engineering, Faculty of Engineering, Mahidol University for their support with facilities.

## 7. References

- [1] Sitthiseripratip, K., Van Oosterwyck, H., Vander Sloten, J., Mahaisavariya, B., Bohez, E.L.J., Suwanprateeb, J. Van Audekercke, R. and Oris P. (2003). Finite element study of trochanteric gamma nail for trochanteric fracture. *Med Eng&Phy*, vol. 25, pp. 99-106.
- [2] Serala, B., Garc, J.M., Cegon, J., Doblare, M. and Serala, F. (2004). Finite element study of intramedullary osteosynthesis in the treatment of trochanteric fractures of the hip: Gamma and PFN. *J. Care Injured*, vol. 35, pp. 130-135.
- [3] Mahaisavariya, B., Sitthiseripratip, K. and Suwanprateeb, J. (2006). Finite element study of the proximal femur with retained trochanteric gamma nail and after removal of nail. *J. Care Injured*, vol. 37, pp. 778-785.
- [4] Aroonjarattham, P., Aroonjarattham, K. and Suvanjumrat, C. (2014). Effect of mechanical axis on strain distribution after total knee replacement. *J. Kasetsart (Nat. Sci.)*, vol. 48(2), pp. 263-282.
- [5] Aroonjarattham, P., Aroonjarattham, K. and Chanasakulniyom, M. (2015). Biomechanical effect of filled biomaterials on distal Thai femur by finite element analysis. *J. Kasetsart (Nat. Sci.)*, vol. 49(2), pp. 263-276.
- [6] Senalpati, S.K. and Pal, S. (2002). Uhmwpe-alumina ceramic composite, an improved prosthesis material for an artificial cement hip joint. *Trends Biomater: Artif. Organs*, vol. 16(1), pp. 5-7.
- [7] Peraz, A., Mahar, A., Negus, C., Newton, P. and Impelluso, T. (2008). A computational evaluation of the effect of intramedullary nail material properties on the stabilization of simulated femoral shaft fracture. *Med Eng & Phys*, vol.30, pp. 755-760.
- [8] El' Sheikn, H.F., MacDnald, B.J. and Hashmi, M.S.J. (2003). Finite element simulation of the hip joint during stumbling: a comparison between static and dynamic loading. *Journal of Material Processing Technology*, vol. 143-144, pp. 249-255.
- [9] Bregmann, G. (2001). "HIP98", Free University, Berlin.
- [10] Heller, M.O., Bergmann, G., Kassi, J.P., Cales, L., Haas, N.P. and Duda, G.N. (2005). Determination of muscle loading at the hip joint for use in pre-clinical testing. *J Biomech*, vol. 38, pp. 1155-1163.
- [11] University of Texas Arlington. Exercise Adaptations to Biological Tissues. (2013). URL:<http://www.uta.edu/faculty/ricard/Classes/KINE3301/Notes/Lesson-15.html>, accessed on 05/08/2015.
- [12] Frost, H.M. (1994). Wolff's law and bone's structural adaptation to mechanical usage: an overview for clinicians. *The Angle Orthodontist*, vol. 64(3), pp.175-188.
- [13] Frost, H.M. (2003). Update of Bone Physiology and Wolff's Law for Clinicians. *The Angle Orthodontist*, vol. 74, pp. 3-15.
- [14] Park, J. and Lakes, R.S. (2007). Biomaterials: an introduction. Springer.

## POS0011

[15] Hamidi, E., Fazeli, A., Yajid, A.Z.M. and Sidik, N.A.C. (2015). Materials Selection for Hip Prosthesis by the Method of Weighted Properties. *Journal of Advanced Research in Materials Science*, vol.4, pp. 1-9.

[16] Black, J. and Hastings, G. (1998). Handbook of Biomaterials Properties, Chapman & Hall, UK.